Revista Brasileira de Ciência do Solo

Division - Soil in Space and Time | Commission - Soil Genesis and Morphology

Hardening and Stability of Plinthic Materials of the Araguaia River Floodplain under Different Drying Treatments

Angélica Pires Batista Martins[(1)], Glenio Guimarães Santos[(2)*], Virlei Álvaro de Oliveira[(3)], Deyvid Diego Carvalho Maranhão[(4)] and Leonardo Santos Collier[(5)]

[(1)] Universidade Federal de Goiás, *Campus* Samambaia, Escola de Agronomia, Departamento de Solos, Programa de Pós-Graduação em Agronomia (Solo e Água), Goiânia, Goiás, Brasil.
[(2)] Universidade Federal de Goiás, *Campus* Samambaia, Escola de Agronomia, Departamento de Solos, Goiânia, Goiás, Brasil.
[(3)] Instituto Brasileiro de Geografia e Estatística, Unidade Estadual de Goiás, Goiânia, Goiás, Brasil.
[(4)] Universidade Federal Rural do Rio de Janeiro, Departamento de Solos, Programa de Pós-Graduação em Agronomia (Ciências do Solo), Seropédica, Rio de Janeiro, Brasil.
[(5)] Universidade Federal de Goiás, *Campus* Samambaia, Escola de Agronomia, Departamento de Solos, Goiânia, Goiás, Brasil.

ABSTRACT: Plinthite and petroplinthite occur frequently in Brazilian soils, but there is little information on the behavior of these materials. The aim of the present study was to assess the effect of different drying periods on the hardening and stability of plinthic materials of soils in the floodplain of the Araguaia River and the João Leite stream in Goiás. Soil samples were collected, with the aid of 0.10 m high and 0.15 m diameter PVC cylinders, directly from the plinthic horizons of five profiles of *Plintossolos Argilúvicos* (Plinthosols). Plinthite and soil matrix subsamples were obtained from these samples. Homogeneous petroplinthite samples were collected from the concretionary horizon of a *Plintossolo Pétrico* (Plinthosol) profile, and these were separated into subsamples with the aid of a rock hammer. All subsamples were dried in two manners: air drying and drying in a forced ventilation oven for 10, 20, 40, 80, and 160 days. Compressive strength and degree of stability were assessed. The results show a considerable variety of responses to the compressive force applied to the plinthite and petroplinthite samples in the same horizon and among the different profiles examined.

Keywords: deterioration of soil structure, dryness, hardness, iron oxide, plinthite.

*** Corresponding author:**
E-mail: gleniogm@gmail.com

Received: June 9, 2017

Approved: December 21, 2017

How to cite: Martins APB, Santos GG, Oliveira VA, Maranhão DDC, Collier LS. Hardening and stability of plinthic materials of the Araguaia River floodplain under different drying treatments. Rev Bras Cienc Solo. 2018;42:e0170190.
https://doi.org/10.1590/18069657rbcs20170190

INTRODUCTION

Plinthite is a formation consisting of a mixture of clay material that is low in organic carbon and rich in iron, or iron and aluminum, with grains of quartz and other minerals (Santos et al., 2013). Plinthite genesis is associated with seasonal changes in groundwater level, as follows: a high groundwater level results in iron content reduction, mobilization, transport, and concentration; low groundwater levels result in irreversible hardening of plinthite, forming nodules or ferruginous concretions called petroplinthites (Moreira and Oliveira, 2008).

Brazil has extensive areas of soils prone to the formation of plinthites and petroplinthites (Anjos et al., 1995; Batista and Santos, 1995). Seasonal groundwater variations make agricultural management of plinthic soils quite complex, requiring control of their water dynamics (IBGE, 2015). In agricultural areas, artificial drainage is required in soils under intensive use. However, excessive lowering of groundwater leads to plinthite hardening (Martins et al., 2006).

Iron oxides strongly influence the hardening of ferruginous materials (Santos and Batista, 1996) and the formation and stabilization of soil structure (Momoli and Cooper, 2016). Determination of hardness, expressed by the compressive strength of the material, allows identification of the degree of hardening and the stage of development of the ferruginous material (Coelho et al., 2001). Regarding stability, Daniels et al. (1978) and Coelho et al. (2001) assessed the conservation of the plinthite structure using wet sieving in soils of the southeast of the United States and north of the state of São Paulo, respectively.

Knowledge of the amount and degree of hardening and structural stability of ferruginous materials is key to proper management of soil used for agricultural production purposes. The presence of plinthite and petroplinthite may affect soil properties such as density, water holding capacity, infiltration, erodibility, soil volume utilized by roots, cation exchange capacity, texture, and structure, which affect not only the hydrological behavior, but also the crop yield of soils (Coelho et al., 2001).

Important information about the time required for the hardening and improvement of structural stability of ferruginous materials after exposure to dryness is not found in the specialized literature. Therefore, the aim of the present study was to assess the hardening and stability of plinthic materials present in soils of the Araguaia River floodplain under different drying treatments for different periods to help improve the classification of ferruginous materials.

MATERIALS AND METHODS

The study was conducted in five soil profiles located in (P1, P2, P3, and P4) and near (P5) the Araguaia River floodplain in Luiz Alves, a district of São Miguel do Araguaia, Goiás (Table 1), because these soils contain plinthite and petroplinthite (*Plintossolos* - Brazilian Soil Classification System; Plinthosols in the World Reference Base of Soil Resources), according to the soil map of the region - Project Radambrasil (Brasil, 1981). For comparison of plinthic materials, material from a soil profile in the municipality of Terezópolis de Goiás (P6), state of Goiás, in the floodplain of the João Leite stream, about twenty kilometers from Goiânia, Goiás, was also examined.

The profiles were selected through field observation and were described according to the recommendations of the Manual of Field Soil Description and Collection (Santos et al., 2015) and the Technical Pedology Manual (IBGE, 2015). The soils investigated were classified according to the Brazilian Soil Classification System (Santos et al., 2013) and World Reference Base for Soil Resources (WRB, 2015).

Table 1. Location of the profiles and characterization of the study sites

Profile	Location	Altitude	Geology[1]	Original material[1]	Local relief	Current use
		m				
P1	13° 14' S 50° 32' W	221	Sedimentary Cover of Bananal	Alluvial sediments	Flat	Natural vegetation
P2	13° 10' S 50° 31' W	220	Sedimentary Cover of Bananal	Alluvial sediments	Flat	Soybean crop
P3	13° 12' S 50° 31' W	220	Sedimentary Cover of Bananal	Alluvial sediments	Flat	Natural vegetation
P4	13° 07' S 50° 30' W	222	Sedimentary Cover of Bananal	Alluvial sediments	Flat	Natural vegetation
P5	13° 15' S 50° 31' W	225	Estrondo Group	Weathering of mica-schist with grenade and sericite schist	Mildy rolling	Natural vegetation
P6	16° 28' S 49° 06' W	753	Anápolis-Itauçu Complex	Colluvial-alluvial sediments	Mildy rolling	Pasture

[1] Project Radambrasil (1981).

Among the floodplain soils affected by seasonal variation of the groundwater, P1 and P3 profiles are the most typical and common soils, while P2 and P4 profiles are probably located on paleo-channels due to their different physical nature (mean texture) (Table 2). Profile P5 has good natural drainage because it is located outside the floodplain.

The climate of the regions is type Aw, defined as tropical with a dry season in winter, according to the Köppen-Geiger classification system. The average annual rainfall is from 1,800 to 2,000 mm and average annual temperature range is from 25 to 26 °C in Luiz Alves, and from 1,200 to 1,400 mm and 22 to 23 °C in Terezópolis de Goiás (Cardoso et al., 2014).

To allow uniformity (volume) and absence of deformation, field samples were collected using 0.10 m high and 0.15 m diameter PVC cylinders, inserted directly into the plinthic horizons, with fifteen replicates (three PVC cylinders for each saturation time period of 40, 80, 120, 160, and 200 days) per profile, according to the following criteria:

In P1 - containing a plinthic horizon, undisturbed samples were collected from the Btf4 and Btf5 horizons at depths ranging from 0.65 to 1.10 m; in P2 - containing a plinthic horizon, undisturbed samples were collected from the 4Btfc2 and 4Btfc3 horizons at depths from 0.61 to 1.10 m; in P3 - containing a plinthic horizon, undisturbed samples were collected from the Btf4 horizon at depths from 1.04 to 1.50 m; in P4 - containing a plinthic horizon, undisturbed samples were collected from the Bf2 horizon at depths from 1.03 to 1.36 m; in P5 - containing a concretionary horizon, three homogeneous samples of petroplinthite were collected in the form of continuous blocks (lateritic concretion "canga"), whose distinguishing criterion was considerable hardness (very hard consistency in the dry sample), with a mean block weight of approximately 400 g per sample, from the Bc1 and Bc2 horizons at depths from 0.09 to 1.03 m; and in P6 - containing a plinthic horizon, undisturbed samples were collected from the Btf1 and Btf2 horizons at depths from 0.41 to 0.76 m.

Subsequently, in a protected environment, soil samples from the PVC cylinders and the P5 petroplinthite samples were placed in plastic containers. Throughout the study period, distilled water was added to the surface of the samples to maintain field moisture. Thus, the samples remained saturated for 40, 80, 120, 160, and 200 days.

After each saturation period, plinthite and soil matrix split-plots (portion without plinthite) from three PVC cylinders per profile were taken at random, with ten replications per drying treatment, according to visual (color) and physical or mechanical (consistency) criteria (IBGE, 2015). In P6, only soil matrix subsamples were collected, which had a reddish colored material characterized as plinthite during soil sample collection in the field, but plinthite could not be distinguished from the soil matrix by hardness.

Table 2. Depth of horizons, grain size composition, and textural class of the profiles investigated

Horizon	Layer	CS	FS	Silt	Clay	TC
	m	g kg^{-1}				
Profile 1 - *Plintossolo Argilúvico Distrófico típico* (Santos et al., 2013)/Plinthosol (WRB, 2015)						
A	0.00-0.17	144	243	202	411	C
E	0.17-0.24	111	262	176	451	C
Btf1	0.24-0.33	104	244	181	471	C
Btf2	0.33-0.45	135	195	198	472	C
Btf3	0.45-0.65	115	218	236	431	C
Btf4	0.65-0.95	121	195	233	451	C
Btf5	0.95-1.10	142	154	232	472	C
Btf6	1.10-1.28^{+}	109	121	256	514	C
Profile 2 - *Plintossolo Argilúvico Eutrófico petroplíntico* (Santos et al., 2013)/Plinthosol (WRB, 2015)						
Ap1	0.00-0.06	29	281	321	369	CL
2Ap2	0.06-0.18	133	448	237	182	SL
3AE	0.18-0.27	175	455	229	141	SL
3EA	0.27-0.34	157	433	249	161	SL
3Efc	0.34-0.50	75	376	327	222	L
3Btfc1	0.50-0.61	71	354	312	263	CL
4Btfc2	0.61-0.76	91	358	329	222	L
4Btfc3	0.76-1.10^{+}	89	366	323	222	L
Profile 3 - *Plintossolo Argilúvico Distrófico típico* (Santos et al., 2013)/Plinthosol (WRB, 2015)						
A	0.00-0.10	162	168	321	349	CL
AE	0.10-0.18	174	162	295	369	CL
E	0.18-0.29	137	230	223	410	C
Btf1	0.29-0.50	111	201	216	472	C
Btf2	0.50-0.75	129	211	189	471	C
Btf3	0.75-1.04	141	203	185	471	C
Btf4	1.04-1.50	117	176	236	471	C
Btf5	1.50-1.70^{+}	92	131	264	513	C
Profile 4 - *Plintossolo Argilúvico Distrófico petroplíntico* (Santos et al., 2013)/Plinthosol (WRB, 2015)						
A	0.00-0.11	42	612	245	101	SL
AE	0.11-0.28	38	586	255	121	SL
Ef1	0.28-0.47	28	542	269	161	SL
Ef2	0.47-0.66	20	513	285	182	SL
Bfc	0.66-0.84	26	469	323	182	L
Bf1	0.84-1.03	20	448	330	202	L
Bf2	1.03-1.36	20	493	204	283	SCL
Btf1	1.36-1.71	59	366	229	346	CL
Btf2	1.71-1.98	37	225	370	368	CL
2Bf	1.98-2.55^{+}	14	287	412	287	CL
Profile 5 - *Plintossolo Pétrico Concrecionário típico* (Santos et al., 2013)/Plinthosol (WRB, 2015)						
Apc	0.00-0.09	154	395	167	284	SCL
Bc1	0.09-0.56	102	285	165	448	C
Bc2	0.56-1.03^{+}	138	297	118	447	C
Profile 6 - *Plintossolo Argilúvico Eutrófico típico* (Santos et al., 2013)/Plinthosol (WRB, 2015)						
Ap	0.00-0.17	319	272	123	286	SCL
AB	0.17-0.27	357	304	74	265	SCL
BAf	0.27-0.41	330	240	102	328	SCL
Btf1	0.41-0.57	282	228	99	391	SC
Btf2	0.57-0.76	211	174	118	497	C
Btf3	0.76-1.03	147	193	120	540	C
Btf4	1.03-1.20	145	195	162	498	C
2Bf1	1.20-1.40	255	323	136	286	SCL
2Bf2	1.40-1.63	283	244	124	349	SCL
2Cgf	1.63-1.75^{+}	190	221	156	433	C

Coarse sand, fine sand, silt, and clay determined by densimeter method (Donagema et al., 2011). CS = coarse sand; FS = fine sand; TC = textural class; C = clay; SL = sandy loam; CL = clay loam; L = loam; SCL = sandy clay loam; SC = sandy clay.

Because of the irregular shape of plinthite and petroplinthite, their subsamples were standardized. Thus, they were measured using a digital caliper in three dimensions (height, width, and length) to calculate the approximate volume of each sample. In turn, in standardization of the soil matrix subsamples, volumetric rings of equal volume (0.02 m in height and 0.02 m in diameter) were used for the material collected in the three PVC cylinders. The plinthite subsamples were manually separated according to visual (color) and physical or mechanical (consistency) criteria (IBGE, 2015), and compression tests with load were used to determine the force required to rupture the subsamples in their original condition after a forty-day period of saturation of the samples in distilled water. Likewise, the petroplinthite samples were separated from each initial block weighing 400 g (collected from the concretionary horizon of profile 5), in subsamples with an average volume of approximately 7 cm^3, with the aid of a rock hammer, with ten replications per treatment; and the force required to rupture the subsamples, also in their original condition after a forty-day period of saturation of the samples in distilled water, was tested.

The plinthite, soil matrix, and petroplinthite subsamples that remained saturated for 40, 80, 120, 160, and 200 days were dried in the air and in a laboratory oven for 160, 80, 40, 20, and 10 days. In a natural environment, the subsamples were placed in plastic containers that did not obstruct water passage in a protected environment that had a mean temperature of 23.7 °C and relative humidity of 64.1 %, according to data obtained from the meteorological station of the UFG School of Agronomy (Figure 1). In the oven, the subsamples were placed in aluminum containers and kept at a constant temperature of 40 °C.

The compressive strength and degree of stability of plinthite, soil matrix, and petroplinthite subsamples were assessed for each treatment. Because of the high variability among the materials of the same horizon (very non-uniform populations), a selective mean was used for assessment purposes, after exclusion of 30 % of the data most dispersed from the overall mean.

The compressive strength of plinthite, soil matrix, and petroplinthite subsamples was assessed with the use of universal mechanical testing equipment (Instron®, model 3367, Grove City, USA) with a 30 kilonewton (kN) load cell. The maximum force, expressed in newtons (N), was reached when the equipment deformed constantly, 40 % compared to the initial height of the material, at a speed of 0.50 mm s^{-1}. Because the material is

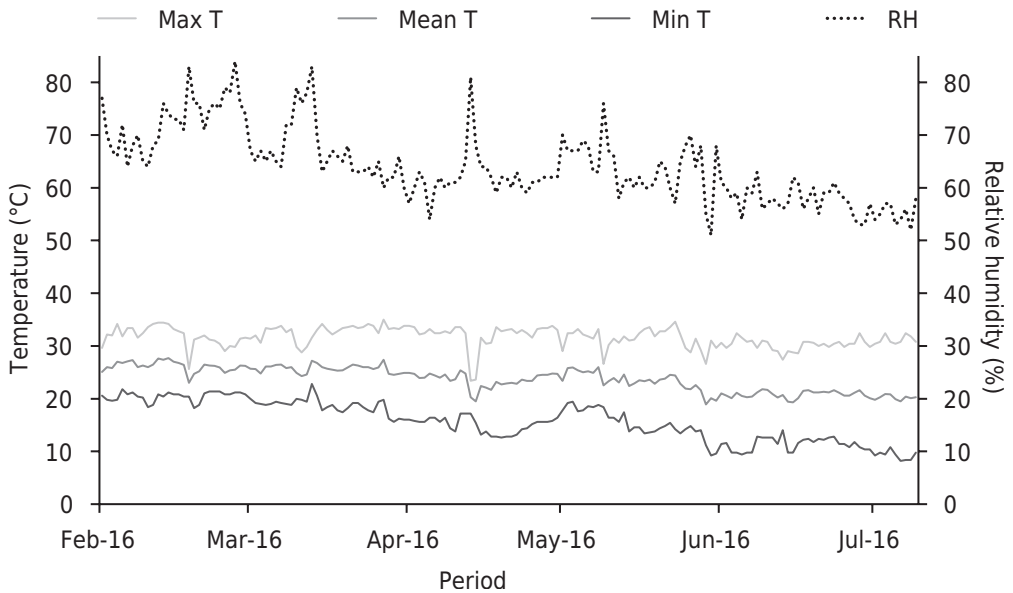

Figure 1. Data of maximum, mean, and minimum temperature and relative humidity during the period studied.

ruptured after compression tests, different batches of subsamples were used for each treatment, i.e., the material used for drying during the first ten days was discarded at the end of the tests, and the same occurred with the subsamples of the other treatments. Compression test values were expressed in N (corresponding to the force required to cause deformation in each subsample, depending on its volume) and N cm^{-3} (force applied per volume of 1 cm^3 in each subsample).

The degree of proportional stability of plinthite and petroplinthite subsamples was analyzed through wet sieving on a Yoder shaker apparatus (Donagema et al., 2011). The subsamples were individually weighed on a semi-analytic scale, pre-moistened by capillarity, placed on moist filter paper, transferred to two sets of five sieves with 2.00, 1.00, 0.50, 0.25, and 0.106 mm diameter openings and mixed vertically in water containers for fifteen minutes (forty cycles per minute). The material retained in each sieve was transferred to aluminum containers and dried in a laboratory oven at 105 °C. Next, the weight and percentage of stable materials in each diameter class were calculated.

To facilitate characterization of the plinthite, soil matrix, and petroplinthite, qualitative-quantitative analysis of the chemical composition of representative samples of these materials was determined by X-ray fluorescence spectrometry using the EDX-700 HS Energy Dispersive X-ray Spectrometer. This analysis was based on pressed pellets made from individual samples of plinthite, soil matrix, and petroplinthite from each horizon of each profile assessed. In the plinthic horizons of the profiles P1, P2, P3 and P4, an individual sample of plinthite and another of soil matrix were analyzed; a sample of petroplinthite belonging to the concretionary horizon of P5; and a soil matrix sample belonging to the plinthic horizon of P6. The individual samples (each individual plinthite, soil matrix, and petroplinthite sample was composed of ten simple samples, per horizon, of each profile) were ground into powder in an agate mortar and pestle, homogenized, and pelletized; they were then compacted for 1 minute with the use of a 5-ton capacity hydraulic press device. The pressed pellets were analyzed in an EDX-700 HS Energy Dispersive X-ray Spectrometer. The selected operating conditions were collimator - 10 mm, vacuum atmosphere, tube voltage - 50 kV, pipe current - automatic µA, irradiation time - 100 s, acquisition mode - quantitative/FP, and analytical line - Kα.

In order to compare the compressive strength of the material in its original condition and after the drying treatments, ten replicates of plinthite, soil matrix, and petroplinthite in each profile were assessed under air-dried and oven-dried conditions. For the subsamples of plinthite and petroplinthite in their original condition forty days after saturation in distilled water, thirty replicates of each material were assessed per profile, to check for correlation between the force applied and the volume (cm^3) of the ferruginous materials. Second-order polynomial regression was used to fit the models. This regression was also used to detect a possible correlation between the mean values of the compressive force applied to the plinthites analyzed in the P1, P2, P3, and P4 plinthic profiles and the percentage values of iron (Fe_2O_3) obtained by X-ray fluorescence spectrometry (XRF).

The mean values of dispersion, stability, and compressive strength of a total of 500 subsamples, 250 of plinthite and 250 of petroplinthite, were determined. Comparisons were made using non-parametric statistics. A mean confidence interval (CI) was 95 % ($p<0.05$), and a standard error of the mean (± SE) was used to verify the reliability of the mean of the calculated sample, through use of the software Xlstat (Addinsoft, 2016). The figures and tables were made with Microsoft Excel 2010 software, and analysis of variance was performed to obtain the F values ($p<0.05$) for each second-order polynomial regression graph.

RESULTS AND DISCUSSION

Morphological aspects and compressive force applied to subsamples of plinthite and petroplinthite under original conditions (before drying)

During morphological description of the soil profiles in the field, a great variability in the hardness of the plinthic materials in the soils investigated was detected, even among samples from the Araguaia River floodplain (P1, P2, P3, and P4). In P1 and P3 - most plinthites of the horizons collected from both profiles were soft when manually examined. In P2 - the consistency of most plinthites of the collected horizons ranged from soft to hard when manually examined. At some points of the plinthic horizon, the presence of large blocks of lateritic concretion was observed in P2. In P4 - the consistency of most plinthites of the collected horizon ranged from soft to hard when manually examined. In the upper portion of the Bfc horizon of the profile, the presence of considerably hardened iron concretions was observed, whereas in the lower portion of the Btf2, only plinthites in the soft stage were observed. In P5 - petroplinthite only occurred in an amount greater than 50 % and with a thickness greater than 0.30 m in the concrete diagnostic horizon. In P6 - although the presence of plinthite in excess of 15 % with a thickness of 0.15 m or more was observed in the field, plinthite could not be distinguished from the soil matrix by hardness, indicating a recent formation process for this material.

Figure 2 shows the results of the compressive force applied related to the volume of plinthite and petroplinthite subsamples of the profiles investigated, under natural conditions. The use of higher force on these ferruginous materials was not associated with their volume, as indicated by the high data dispersion (low R^2 values). In general, there was considerable variation in the load applied to the plinthites of profiles P1, P2, P3, and P4 and to the petroplinthite of P5 (Figure 2a), despite the fact that this material is present in soils at more advanced stages of maturity.

Although the Araguaia River floodplain is uniform in several aspects, such as climate and relief, the variability of forces applied to the profiles is caused by the different formation microenvironments, such as the internal areas of paleo-channels and anthropic influence. However, differences are mostly due to the fact that the plinthite formation is derived from the concentration of material segregated and transported from adjacent sites of the profile, a mechanism that depends on many regulatory factors, such as redox potential, diffusion, ionic nature, and water dynamics.

The highest compressive strengths were observed in the plinthites of the P2 and P4 profiles (Figures 2c and 2e) and in the P5 petroplinthite (Figure 2f), whereas the lowest values were observed for the plinthites of the P1 and P3 profiles (Figures 2b and 2d), which can, at least partially, be attributed to the iron content of the materials (Table 3). Therefore, determination of the chemical composition of the materials investigated revealed that the plinthite and petroplinthite subsamples that required higher compressive forces had the highest total iron contents. Moreover, for the plinthic horizons of the Araguaia River floodplain, as shown by the second-order polynomial equation of figure 3 ($R^2 = 0.9969$), the results confirmed that the compressive strength required to deform plinthite increases with an increase in the percentages of Fe_2O_3 in the material under study.

In the petroplinthite of the P5 profile, the total iron content was much higher than in the plinthites of the other profiles, highlighting the key role of iron compounds in the increase in compressive strength of ferruginous materials. As reported by Santos and Batista (1996), the hardening of ferruginous materials is related to the increase in iron content and the higher degree of crystallinity of iron.

The results obtained in the compression tests are consistent with field observations, in which the plinthites of the P2 and P4 profiles were morphologically more hardened. Thus, these profiles were relatively more mature than P1 and P3, and, hence, the plinthites of the P2 and P4 profiles were formed and subjected to at least partial dryness to allow the higher compression force.

The profile P2 differs from P4 because it is located in a slightly lower area (Table 1) and is currently subject to less drainage. It is believed that anthropic intervention (the area has been cultivated for approximately ten years) may be contributing to the significant plinthite hardening, which occurs in association with soft material. In P2, there were sites with large lateritic concretions, in which all the material of the horizon (matrix and plinthite) is cemented, even when groundwater level is high. The lower initial hardening of the plinthites of the P1 and P3 profiles is a result of the lower iron content and the more recent formation process. These profiles are located in low areas subject to typical seasonal flooding of the plain, and thus were not exposed to severe dryness that might cause greater hardening. Consequently, less force was required for compression of the material.

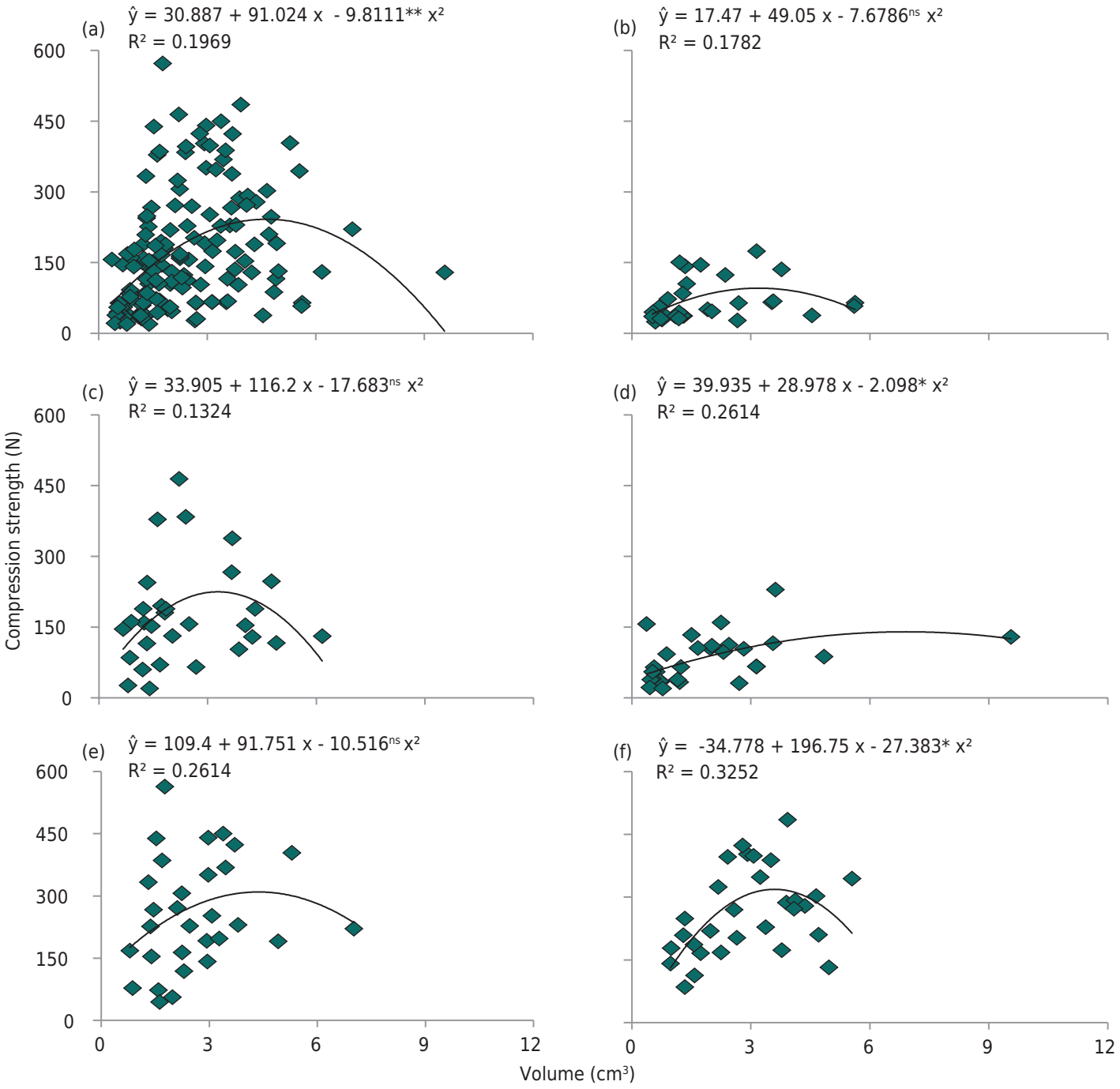

Figure 2. Correlation between the values of compressive strength and the volume of plinthite and petroplinthite of the profiles studied, under natural conditions. Profiles P1-P5 (a); profile 1 (b); profile 2 (c); profile 3 (d); profile 4 (e); and profile 5 (f). ^{ns} = not significant; * = significant at 5 % probability; ** = significant at 1 % probability by the F test.

Table 3. Main chemical components of plinthite (PL), soil matrix (SM), and petroplinthite (PP) determined by X-ray fluorescence spectrometry (XRF) for each profile examined

Material	SiO_2	Al_2O_3	Fe_2O_3	TiO_2	MgO	K2O	V_2O_5	Z_rO_2
	%							
Profile 1 - *Plintossolo Argilúvico Distrófico típico* (Santos et al., 2013)/Plinthosol (WRB, 2015)								
PL	44.81	35.40	17.51	1.16	n.d.	1.01	0.06	0.05
SM	50.85	38.87	7.49	1.53	n.d.	1.14	n.d.	0.06
Profile 2 - *Plintossolo Argilúvico Eutrófico petroplíntico* (Santos et al., 2013)/Plinthosol (WRB, 2015)								
PL	55.53	21.81	21.23	0.98	n.d.	n.d.	0.05	0.08
SM	73.07	21.71	2.47	1.12	0.86	0.67	n.d.	0.10
Profile 3 - *Plintossolo Argilúvico Distrófico típico* (Santos et al., 2013)/Plinthosol (WRB, 2015)								
PL	50.58	30.15	15.85	1.22	1.04	1.02	n.d.	n.d.
SM	58.03	32.84	5.26	1.43	1.34	1.07	n.d.	n.d.
Profile 4 - *Plintossolo Argilúvico Distrófico petroplíntico* (Santos et al., 2013)/Plinthosol (WRB, 2015)								
PL	56.71	19.29	22.93	0.93	n.d.	n.d.	0.06	0.07
SM	76.03	19.80	1.34	1.15	0.76	0.67	n.d.	0.10
Profile 5 - *Plintossolo Pétrico Concrecionário típico* (Santos et al., 2013)/Plinthosol (WRB, 2015)								
PP	42.55	17.74	38.77	0.68	n.d.	n.d.	0.13	0.05
Profile 6 - *Plintossolo Argilúvico Eutrófico típico* (Santos et al., 2013)/Plinthosol (WRB, 2015)								
SM	61.95	29.03	3.33	3.55	1.21	0.46	n.d.	0.11

n.d. = not detected

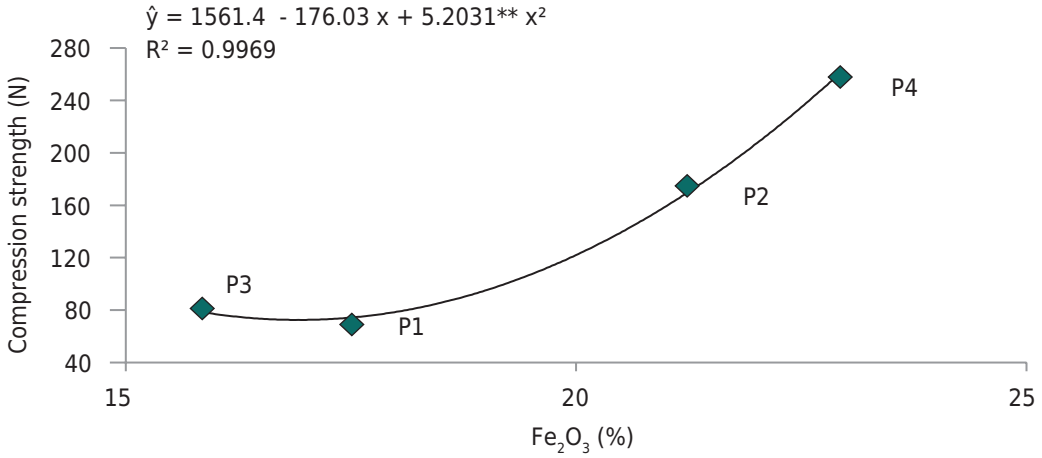

Figure 3. Correlation between the mean values of compressive strength and the percentage values of iron oxide (Fe_2O_3) in plinthites of profiles P1, P2, P3, and P4. ** = significant at 1 % probability by the F test.

In summary, the profiles investigated are distinguished from each other in the formation stage of the plinthites. This diversity is mainly related to changes in the water regime at each site, as well as to intervention in the water regime from anthropic activity (Batista and Santos, 1995).

Differences in the compressive force applied to the plinthites and the petroplinthite could be observed within the same soil profile. This finding indicates that materials at different stages of maturity and of different compositions coexist in the same soil, demonstrating the heterogeneity of the materials examined. According to Coelho et al. (2001), the diversity of plinthic and petroplinthic profiles in the same horizon is due to the association of pedo-, litho-, and biological factors.

It should also be stressed that even in a population with the same behavioral trend, there were variations in the values of compressive force applied. This is more evident in lowland profiles (P1, P2, P3, and P4), where the plinthite in the soils is still in the formation process, i.e., at a more recent maturity stage than the petroplinthite of the P5 profile, which is at a more mature stage and with hardened material. The differences in such cases can mainly be attributed to the time of formation or maturity of the material.

Compressive force applied to subsamples of plinthite and petroplinthite under air-dried and oven-dried conditions

There was no difference in the impact of the different types of drying (air drying and oven drying) on the compressive force applied to the plinthites in the P1, P2, P3, and P4 profiles and in the petroplinthite of P5 (Figure 4). However, higher compressive strength was generally observed in materials dried in the oven than in those dried in the air. The higher temperature and air circulation may have caused greater evaporation of water, which was reflected in the increased compressive strength of the materials. Air circulation together with higher temperature tends to remove the moist air layer around the surface and replace it with drier air, providing a high moisture gradient with increased evaporation capacity (Cavalcanti Júnior et al., 2013). This indicates that the compressive strength of the material may be higher in environments where soil profiles are exposed to higher incidence of sunlight and wind.

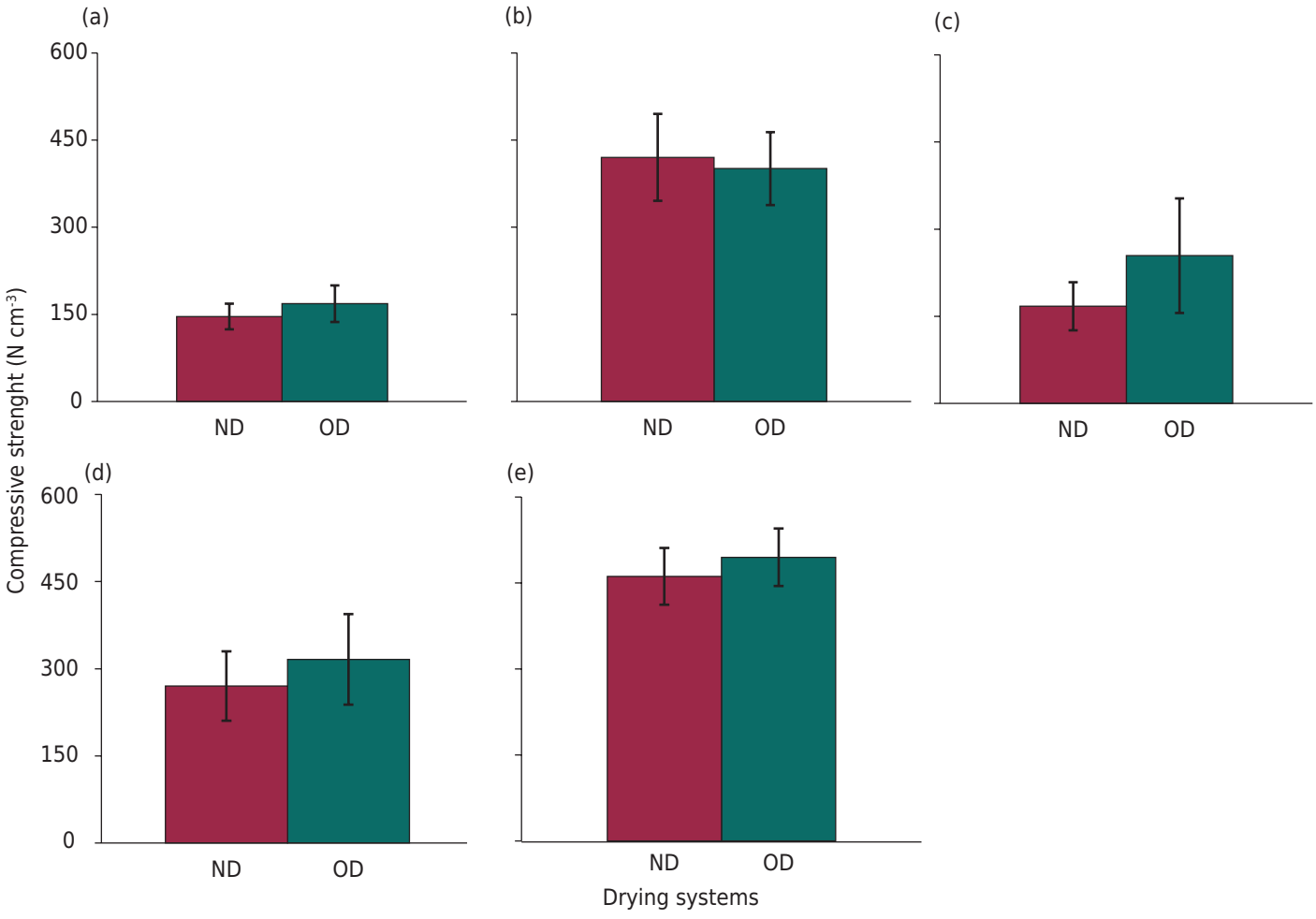

Figure 4. Mean and standard error of the mean compressive strength of plinthite and petroplinthite in the profiles examined, after natural air drying (ND) and oven drying (OD), with a 95 % confidence interval ($p<0.05$). A = profile 1; B = profile 2; C = profile 3; D = profile 4; E = profile 5.

Compressive force applied to plinthite and petroplinthite subsamples in their original condition (before drying), and after natural air drying and oven drying for different periods

There was a general trend of higher values in the compressive force applied to the plinthites of the P1, P2, P3, and P4 profiles and to the P5 petroplinthite in their original condition compared to that of the subsamples that underwent air drying and oven drying (Table 4). Thus, drying is a determining factor of the increase in the compressive force applied. Regarding the behavior of the plinthites of P4, the wide variability in the composition and hence in the degree of maturation of the materials present in this profile produced some changes in the trend mentioned – a decrease in compressive strength was observed after 160 days of air drying of the subsamples, whereas in oven drying, there was a decrease in compressive strength after 80 days, contrasting with the natural trend observed in the other profiles.

The P4 profile differs from the other floodplain profiles in its current slightly drier water regime. As this profile is located in a different slightly higher site (a sort of paleo-channel), the possibility of remobilization of concretionary material (previously hardened plinthite) at the deposition site can be affirmed. Thus, the upper part of the profile has very hardened iron concretions, and the lower part has softer (less hardened) plinthites, with poor drainage, and therefore, in a more recent stage of formation. This combination of formation stages determined by differences in drainage may have favored the occurrence of such a wide variety in the hardness of the materials in the horizon.

Table 4. Mean value and standard error of the average compressive strength of the plinthites and the petroplinthite of the profiles examined, in natural condition and after air drying and oven drying, for different periods

Material	Period	Profile 1	Profile 2	Profile 3	Profile 4	Profile 5
		Strength[1]				
	day	N cm^{-3}				
		Natural condition				
		45.38 ± 2.57[2]	94.05 ± 4.24	58.51 ± 6.89	121.32 ± 4.37	268.17 ± 8.53
		Air drying				
Plinthite	10	163.04 ± 19.65	524.29 ± 70.19	173.15 ± 19.66	298.65 ± 20.45	n.a.[3]
Plinthite	20	131.52 ± 10.84	450.53 ± 113.94	162.21 ± 13.98	333.05 ± 56.09	n.a.
Plinthite	40	151.33 ± 19.57	497.67 ± 37.50	69.00 ± 9.90	406.77 ± 91.12	n.a.
Plinthite	80	159.21 ± 39.18	216.52 ± 36.91	101.67 ± 17.03	232.39 ± 46.87	n.a.
Plinthite	160	126.61 ± 27.33	412.66 ± 88.47	329.84 ± 63.68	78.38 ± 10.34	n.a.
Petroplinthite	10	n.a.	n.a.	n.a.	n.a.	532.93 ± 43.22
Petroplinthite	20	n.a.	n.a.	n.a.	n.a.	478.79 ± 43.98
Petroplinthite	40	n.a.	n.a.	n.a.	n.a.	514.45 ± 66.69
Petroplinthite	80	n.a.	n.a.	n.a.	n.a.	296.57 ± 47.56
Petroplinthite	160	n.a.	n.a.	n.a.	n.a.	485.61 ± 19.66
		Oven drying				
Plinthite	10	221.35 ± 16.41	511.37 ± 39.81	168.41 ± 24.94	639.48 ± 85.62	n.a.
Plinthite	20	166.86 ± 41.40	184.60 ± 45.36	116.70 ± 32.02	332.00 ± 52.58	n.a.
Plinthite	40	117.29 ± 12.90	393.95 ± 48.08	150.33 ± 42.33	344.07 ± 42.79	n.a.
Plinthite	80	229.26 ± 48.10	542.47 ± 64.28	668.69 ± 160.22	113.91 ± 19.43	n.a.
Plinthite	160	107.14 ± 13.77	372.22 ± 60.21	167.11 ± 39.40	151.16 ± 20.89	n.a.
Petroplinthite	10	n.a.	n.a.	n.a.	n.a.	374.86 ± 40.67
Petroplinthite	20	n.a.	n.a.	n.a.	n.a.	585.19 ± 64.14
Petroplinthite	40	n.a.	n.a.	n.a.	n.a.	563.66 ± 25.94
Petroplinthite	80	n.a.	n.a.	n.a.	n.a.	468.38 ± 76.58
Petroplinthite	160	n.a.	n.a.	n.a.	n.a.	482.76 ± 16.41

[1] The compressive strength of plinthite and petroplinthite subsamples was assessed with the use of universal mechanical testing equipment (Instron®, model 3367, Grove City, USA) with a 30 kilonewton (kN) load cell.[2] 95 % confidence interval ($p<0.05$).[3] n.a. = not analyzed.

Despite the impact of the types of drying on the compressive strength of plinthite and petroplinthite, the drying periods could not be properly assessed in this study because the compression tests were not applied to the same population or "batch" of subsamples in all the drying treatments due to the impossibility of reusing subsamples from previous periods in subsequent periods after their rupture or fragmentation. Thus, the different compressive strengths among the samples that were air dried and oven dried for different periods are mainly due to sampling variation (collection of samples from different layers of the same horizon), to chemical composition, and to the initial stage of hardening of the materials in the field (degree of maturation). Apparently, the differences in plinthite formation, development, and hardening are explained by the increase in iron and aluminum concentration, which occurs by absolute concentration associated with relative concentration, through the loss of other elements (Driessen and Dudal, 1991).

Compressive force applied to matrix subsamples under air drying and oven drying for different periods

In general, there was no difference in the impact of the two types of drying (air and oven) on the compressive force applied to the matrix of the horizons of all the profiles (Figure 5). This is mainly due to the low iron content in the matrix compared to plinthite (Table 3), which is the main cementing agent of these materials.

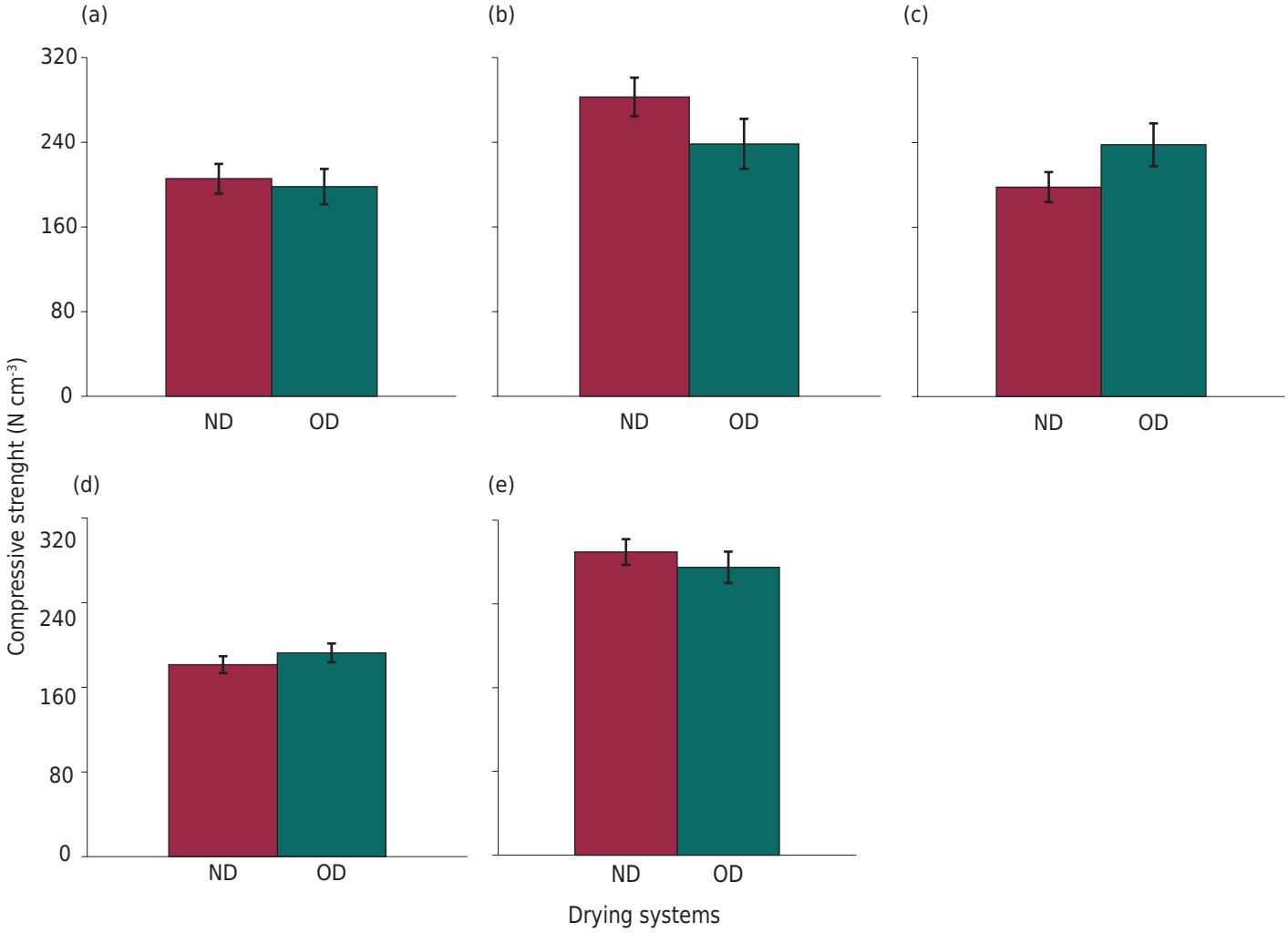

Figure 5. Mean value and standard error of the mean compressive strength of the matrix material of horizons of the soil profiles examined after natural air drying (ND) and oven drying (OD), with a 95 % confidence interval ($p<0.05$). A = profile 1; B = profile 2; C = profile 3; D = profile 4; E = profile 6.

In general, the compressive force applied to the subsamples of the matrix of the horizons of all the profiles in original condition (before drying) increased compared to the force applied to the subsamples subjected to air drying and oven drying (Table 5). Although the total iron contents are low in comparison to plinthite, and iron is generally found in non-crystalline form (Miguel et al., 2013), not solubilized or in the molecules of some minerals, it is believed that the aluminum present in the material increases the compressive strength of the material, by substituting the iron in the iron oxides molecules (Ker, 1997; van Wambeke, 2002).

There was little variability in the values of compressive force applied to the matrix of the horizons of the same profile as a consequence of the increase in the periods of natural air drying and oven drying. This result demonstrates that drying time does not influence the gradual increase in compressive strength, possibly due to the process of iron migration to the plinthite layers, as evidenced in the lower iron content in the matrix than in the plinthite of the profiles investigated (Santos and Batista, 1996; Duarte et al., 2000). Furthermore, it was found that the compressive forces applied to the different profiles do not differ much among themselves. Thus, although some profiles show negligible iron content in the matrix (Table 3), such as profiles P2, P4, and even P6, which is not located in the Araguaia River flood plain, the applied compressive force remains stable, with few variations among the profiles. This fact corroborates the lack of association between iron content and the increase in compressive force applied to the matrix, contrasting with the association of iron content and compressive force applied to plinthite and petroplinthite.

The plinthic horizon matrix of the P2 and P6 profiles required higher compressive strength compared to the other subsamples assessed, in response to the air and oven drying treatments. Although the matrix of these profiles had low total iron contents compared to the P1 and P3 profiles (Table 3), it had very significant contents of total aluminum, which may contribute to increasing the stabilization of iron oxides through isomorphous substitution, probably in compounds like goethite (Ker, 1997; van Wambeke, 2002). However, more in-depth studies are needed regarding the contribution of aluminum to an increase in compressive strength through isomorphous substitution of Fe for Al in iron oxides.

Table 5. Mean value and standard error of the averagecompressive strength of the matrix material of horizons of the profiles examined, after air drying and oven drying for different periods

Material	Period	Profile 1	Profile 2	Profile 3	Profile 4	Profile 6
		Strength[1]				
	day	N				
Natural condition						
		27.17 ± 0.75[2]	51.42 ± 0.82	13.53 ± 1.03	36.10 ± 1.16	35.93 ± 0.66
Air drying						
Matrix	10	199.87 ± 9.75	283.72 ± 17.98	186.66 ± 11.35	199.44 ± 4.95	276.79 ± 4.78
Matrix	20	199.97 ± 9.34	348.80 ± 15.07	183.69 ± 3.79	172.02 ± 6.72	278.51 ± 11.73
Matrix	40	216.91 ± 8.59	284.70 ± 16.47	177.37 ± 15.36	165.83 ± 3.87	293.94 ± 22.63
Matrix	80	159.76 ± 14.83	232.25 ± 12.95	185.11 ± 7.40	189.44 ± 4.25	285.45 ± 11.22
Matrix	160	251.18 ± 11.76	264.53 ± 8.94	256.64 ± 14.78	180.31 ± 14.38	313.19 ± 9.38
Oven drying						
Matrix	10	150.98 ± 11.38	180.45 ± 14.74	187.90 ± 16.46	165.67 ± 5.05	226.88 ± 10.18
Matrix	20	199.58 ± 12.17	175.63 ± 8.76	220.17 ± 17.05	203.86 ± 4.36	270.23 ± 11.43
Matrix	40	183.19 ± 17.22	299.40 ± 27.62	234.87 ± 24.74	179.35 ± 11.26	294.96 ± 11.63
Matrix	80	256.11 ± 15.00	281.59 ± 21.60	257.85 ± 19.92	202.56 ± 6.88	272.15 ± 10.37
Matrix	160	200.42 ± 12.19	255.17 ± 10.78	288.57 ± 16.66	211.14 ± 8.78	310.40 ± 20.12

[1] The compressive strength of plinthite and petroplinthite subsamples was assessed with the use of universal mechanical testing equipment (Instron®, model 3367, Grove City, USA) with a 30 kilonewton (kN) load cell. [2] 95% confidence interval ($p<0.05$).

Higher stability of iron oxides seems to be associated with higher aluminum contents (Inda Junior and Kämpf, 2005). Thus, higher aluminum content through isomorphous substitution of iron in goethite confers greater stability than in hematite, with rates of aluminum substitution of 46 % moles of aluminum in goethite and 23 % moles of aluminum in hematite (Ker, 1997).

Stability of subsamples of plinthite and petroplinthite under different types and periods of drying

Regarding stability, it was observed that after air drying and oven drying, the plinthite subsamples of P1, P2, P3, and P4 profiles and the petroplinthite subsample of the P5 profile remained practically unchanged when passed through a 2.00 mm mesh sieve (Table 6). Therefore, the ferruginous materials investigated are highly stable, corroborating studies by Momoli and Cooper (2016), since iron and aluminum oxides are considered cementing agents responsible for high cohesion among the particles, which favors stabilization. In P5, a profile of *Plintossolo Pétrico* with different geneses of all the profiles showed high stability of the petroplinthite, causing less structural damage than in the plinthites of the other profiles. Higher cementation with iron oxides observed in the petroplinthite layer during the hardening process results in a structure more stable than that of the plinthite (Daniels et al., 1978).

There was no impact of the different types of drying (air and oven) on the degree of stability of the plinthite subsamples of the P1 and P4 profiles, contrasting with the other profiles, where such differences were observed; higher stability values were found in the subsamples dried in the oven. These results can likewise be related to higher temperature and air circulation, which results in greater evaporation of humidity and a consequent increase in the structural stability of the material. It should also be emphasized that the finer poorly-structured material was almost entirely retained or it only passed through a sieve of decreased mesh size, characterizing silt (<0.05 mm) or clay (<0.002 mm) material, which is probably a consequence of the poorer structural stability of small, low-resistance portions occurring in the middle of the more cemented/stable material.

Similarly, longer drying times did not affect the degree of stability of the plinthite subsamples of the P1, P2, P3, and P4 profiles and of the petroplinthite sample of the P5 profile (Table 7). The wide variation among the materials examined in this study may have contributed to the absence of behavioral trends. The high stability of the ferruginous materials suggests that further studies on this subject use longer assessment times.

Table 6. Mean value and standard error of the average stability of the plinthites (PL) and the petroplinthite (PP) of the profiles examined, after air drying and oven drying

Profile	Material	>2.00 mm[1]	1.00 mm	0.50 mm	0.25 mm	0.106 mm	<0.106 mm
		Stability[2]					
		%					
		Air drying					
P1	PL	97.11 ± 0.23[3]	0.09 ± 0.05	0.16 ± 0.07	0.20 ± 0.08	1.23 ± 0.19	1.21 ± 0.11
P2	PL	97.75 ± 0.10	0.09 ± 0.04	0.05 ± 0.03	0.11 ± 0.05	1.13 ± 0.14	0.87 ± 0.09
P3	PL	96.86 ± 0.27	0.31 ± 0.08	0.31 ± 0.08	0.32 ± 0.09	1.13 ± 0.18	1.07 ± 0.14
P4	PL	97.67 ± 0.10	0.04 ± 0.03	0.03 ± 0.02	0.18 ± 0.06	1.29 ± 0.12	0.79 ± 0.09
P5	PP	99.06 ± 0.06	0.11 ± 0.03	0.03 ± 0.02	0.12 ± 0.03	0.35 ± 0.06	0.33 ± 0.04
		Oven drying					
P1	PL	97.13 ± 0.43	0.15 ± 0.08	0.36 ± 0.17	0.50 ± 0.16	0.58 ± 0.19	1.28 ± 0.12
P2	PL	98.14 ± 0.08	0.13 ± 0.03	0.15 ± 0.05	0.21 ± 0.05	0.69 ± 0.12	0.68 ± 0.09
P3	PL	98.08 ± 0.09	0.05 ± 0.02	0.19 ± 0.06	0.19 ± 0.05	0.67 ± 0.11	0.82 ± 0.11
P4	PL	97.61 ± 0.22	0.04 ± 0.04	0.12 ± 0.07	0.20 ± 0.09	0.93 ± 0.16	1.10 ± 0.13
P5	PP	99.30 ± 0.05	0.02 ± 0.01	0.02 ± 0.01	0.05 ± 0.02	0.27 ± 0.04	0.34 ± 0.04

[1] Set of sieves. [2] The stability of plinthite and petroplinthite subsamples was analyzed through wet sieving on a Yoder shaker apparatus (Donagema et al., 2011). [3] 95 % confidence interval ($p<0.05$).

Table 7. Mean value and standard error of the average stability of the plinthites (PL) and the petroplinthite (PP) of the profiles examined, after air drying and oven drying for different periods

Profile	Material	Period	>2.00 mm[1]	1.00 mm	0.50 mm	0.25 mm	0.106 mm	<0.106 mm
			Stability[2]					
		day	%					
			Air drying					
P1	PL	10	97.80 ± 0.26[3]	0.00 ± 0.00	0.07 ± 0.07	0.16 ± 0.10	1.09 ± 0.22	0.88 ± 0.15
P1	PL	20	94.76 ± 0.27	0.14 ± 0.14	0.20 ± 0.14	0.61 ± 0.25	2.87 ± 0.35	1.42 ± 0.33
P1	PL	40	97.61 ± 0.28	0.00 ± 0.00	0.20 ± 0.20	0.00 ± 0.00	1.21 ± 0.21	0.98 ± 0.19
P1	PL	80	97.66 ± 0.23	0.00 ± 0.00	0.00 ± 0.00	0.21 ± 0.21	0.84 ± 0.37	1.29 ± 0.22
P1	PL	160	97.72 ± 0.23	0.29 ± 0.21	0.33 ± 0.23	0.00 ± 0.00	0.16 ± 0.16	1.50 ± 0.27
P2	PL	10	98.03 ± 0.17	0.08 ± 0.08	0.07 ± 0.05	0.07 ± 0.05	0.91 ± 0.26	0.84 ± 0.18
P2	PL	20	97.35 ± 0.19	0.00 ± 0.00	0.00 ± 0.00	0.30 ± 0.20	1.68 ± 0.29	0.67 ± 0.09
P2	PL	40	97.43 ± 0.22	0.00 ± 0.00	0.00 ± 0.00	0.00 ± 0.00	1.36 ± 0.40	1.21 ± 0.24
P2	PL	80	98.35 ± 0.16	0.17 ± 0.17	0.00 ± 0.00	0.00 ± 0.00	0.46 ± 0.28	1.02 ± 0.18
P2	PL	160	97.56 ± 0.20	0.18 ± 0.12	0.20 ± 0.11	0.20 ± 0.08	1.22 ± 0.21	0.64 ± 0.22
P3	PL	10	97.00 ± 0.24	0.46 ± 0.20	0.52 ± 0.16	0.32 ± 0.16	0.61 ± 0.13	1.09 ± 0.24
P3	PL	20	97.88 ± 0.31	0.05 ± 0.05	0.14 ± 0.14	0.18 ± 0.12	1.15 ± 0.36	0.60 ± 0.21
P3	PL	40	95.85 ± 0.50	0.53 ± 0.26	0.31 ± 0.23	0.25 ± 0.25	1.26 ± 0.42	1.80 ± 0.44
P3	PL	80	94.88 ± 0.31	0.23 ± 0.11	0.38 ± 0.20	0.65 ± 0.28	2.43 ± 0.33	1.43 ± 0.27
P3	PL	160	98.71 ± 0.06	0.29 ± 0.11	0.17 ± 0.08	0.22 ± 0.11	0.17 ± 0.11	0.44 ± 0.04
P4	PL	10	97.55 ± 0.22	0.00 ± 0.00	0.07 ± 0.07	0.07 ± 0.07	1.09 ± 0.39	1.22 ± 0.36
P4	PL	20	98.43 ± 0.15	0.10 ± 0.10	0.00 ± 0.00	0.27 ± 0.14	0.58 ± 0.22	0.62 ± 0.09
P4	PL	40	97.86 ± 0.11	0.00 ± 0.00	0.00 ± 0.00	0.10 ± 0.10	1.47 ± 0.15	0.57 ± 0.06
P4	PL	80	97.07 ± 0.17	0.00 ± 0.00	0.00 ± 0.00	0.14 ± 0.14	2.00 ± 0.09	0.79 ± 0.09
P4	PL	160	97.44 ± 0.11	0.08 ± 0.08	0.09 ± 0.06	0.32 ± 0.16	1.33 ± 0.15	0.74 ± 0.16
P5	PP	10	98.85 ± 0.07	0.19 ± 0.07	0.14 ± 0.07	0.33 ± 0.10	0.16 ± 0.04	0.33 ± 0.15
P5	PP	20	98.69 ± 0.09	0.00 ± 0.00	0.00 ± 0.00	0.11 ± 0.07	0.94 ± 0.07	0.26 ± 0.02
P5	PP	40	99.07 ± 0.08	0.09 ± 0.09	0.00 ± 0.00	0.06 ± 0.06	0.31 ± 0.13	0.47 ± 0.07
P5	PP	80	99.46 ± 0.11	0.00 ± 0.00	0.03 ± 0.03	0.06 ± 0.04	0.20 ± 0.05	0.25 ± 0.05
P5	PP	160	99.23 ± 0.09	0.30 ± 0.07	0.00 ± 0.00	0.03 ± 0.03	0.09 ± 0.09	0.35 ± 0.08
			Oven drying					
P1	PL	10	92.49 ± 0.61	0.53 ± 0.34	1.56 ± 0.72	2.21 ± 0.32	1.24 ± 0.83	1.97 ± 0.44
P1	PL	20	97.36 ± 0.26	0.00 ± 0.00	0.26 ± 0.17	0.00 ± 0.00	1.20 ± 0.30	1.18 ± 0.19
P1	PL	40	98.48 ± 0.23	0.07 ± 0.07	0.00 ± 0.00	0.28 ± 0.18	0.20 ± 0.15	0.97 ± 0.23
P1	PL	80	98.50 ± 0.16	0.14 ± 0.14	0.00 ± 0.00	0.00 ± 0.00	0.26 ± 0.17	1.10 ± 0.08
P1	PL	160	98.83 ± 0.03	0.00 ± 0.00	0.00 ± 0.00	0.00 ± 0.00	0.00 ± 0.00	1.17 ± 0.03
P2	PL	10	98.30 ± 0.19	0.15 ± 0.04	0.30 ± 0.21	0.18 ± 0.06	0.60 ± 0.26	0.47 ± 0.18
P2	PL	20	97.96 ± 0.09	0.10 ± 0.06	0.12 ± 0.07	0.33 ± 0.17	0.37 ± 0.14	1.12 ± 0.21
P2	PL	40	98.00 ± 0.11	0.08 ± 0.03	0.06 ± 0.04	0.33 ± 0.08	0.35 ± 0.11	1.18 ± 0.15
P2	PL	80	97.94 ± 0.12	0.00 ± 0.00	0.00 ± 0.00	0.07 ± 0.04	1.68 ± 0.18	0.31 ± 0.09
P2	PL	160	98.51 ± 0.28	0.34 ± 0.12	0.24 ± 0.12	0.17 ± 0.13	0.42 ± 0.23	0.32 ± 0.04
P3	PL	10	97.74 ± 0.25	0.01 ± 0.01	0.41 ± 0.25	0.00 ± 0.00	0.20 ± 0.20	1.64 ± 0.22
P3	PL	20	97.67 ± 0.25	0.17 ± 0.06	0.06 ± 0.06	0.37 ± 0.10	1.05 ± 0.33	0.68 ± 0.18
P3	PL	40	98.59 ± 0.07	0.02 ± 0.02	0.00 ± 0.00	0.08 ± 0.05	0.41 ± 0.17	0.90 ± 0.13
P3	PL	80	98.36 ± 0.07	0.00 ± 0.00	0.20 ± 0.13	0.13 ± 0.08	0.73 ± 0.20	0.58 ± 0.17
P3	PL	160	98.07 ± 0.08	0.05 ± 0.05	0.30 ± 0.10	0.39 ± 0.17	0.97 ± 0.20	0.22 ± 0.09
P4	PL	10	95.51 ± 0.45	0.00 ± 0.00	0.32 ± 0.32	0.83 ± 0.36	1.55 ± 0.55	1.79 ± 0.42
P4	PL	20	97.70 ± 0.23	0.19 ± 0.19	0.17 ± 0.11	0.07 ± 0.07	0.93 ± 0.28	0.94 ± 0.27
P4	PL	40	98.18 ± 0.21	0.00 ± 0.00	0.11 ± 0.11	0.09 ± 0.09	0.57 ± 0.26	1.05 ± 0.14
P4	PL	80	98.40 ± 0.38	0.00 ± 0.00	0.00 ± 0.00	0.00 ± 0.00	1.12 ± 0.39	0.48 ± 0.18
P4	PL	160	98.26 ± 0.12	0.00 ± 0.00	0.00 ± 0.00	0.00 ± 0.00	0.45 ± 0.18	1.29 ± 0.17
P5	PP	10	99.51 ± 0.04	0.00 ± 0.00	0.00 ± 0.00	0.00 ± 0.00	0.20 ± 0.06	0.29 ± 0.05
P5	PP	20	99.11 ± 0.06	0.00 ± 0.00	0.00 ± 0.00	0.00 ± 0.00	0.49 ± 0.08	0.40 ± 0.06
P5	PP	40	99.09 ± 0.06	0.05 ± 0.05	0.07 ± 0.05	0.21 ± 0.08	0.37 ± 0.09	0.21 ± 0.02
P5	PP	80	99.63 ± 0.04	0.00 ± 0.00	0.00 ± 0.00	0.00 ± 0.00	0.14 ± 0.06	0.23 ± 0.04
P5	PP	160	99.16 ± 0.12	0.05 ± 0.05	0.03 ± 0.03	0.02 ± 0.02	0.14 ± 0.09	0.60 ± 0.15

[1] Set of sieves. [2] The stability of plinthite and petroplinthite subsamples was analyzed through wet sieving on a Yoder shaker apparatus (Donagema et al., 2011).[3] 95 % confidence interval ($p<0.05$).

CONCLUSIONS

The results show a considerable variety of responses to the compressive force applied to the plinthite and petroplinthite samples in the same horizon and among the different profiles examined.

High iron and/or aluminum contents are associated with increased level of hardness demonstrated in the compressive force applied to plinthite and petroplinthite samples.

The plinthite samples showed increased levels of hardness under different drying conditions.

The assessment of the drying periods of the present study was jeopardized by the wide variability of the materials examined and the impossibility of reusing samples in the compression tests because of rupture or fragmentation.

ACKNOWLEDGMENTS

To Capes for granting a master's degree program scholarship to the first author; to CNPq (Grant No. 457628/2014-6) for financial support; to SiBCS project (Research and innovation to improve the taxonomy of Brazilian soils - Embrapa/SEG 02.14.01.008.00.00) for the chemical and physical analyses made; and to the geology laboratory of UFMT for the analyses by X-ray fluorescence spectrometry.

REFERENCES

Addinsoft. Statistical software & data analysis add-on for Excel. Version 2016.4. Nova York: Addinsoft; 2016.

Anjos LHC, Franzmeier DP, Schulze DG. Formation of soils with plinthite on a toposequence in Maranhão State, Brazil. Geoderma. 1995;64:257-79. https://doi.org/10.1016/0016-7061(94)00022-3

Batista MA, Santos MC. Morfologia e gênese de dois solos com plintita da região meio-norte do Brasil. Rev Bras Cienc Solo. 1995;19:287-96.

Brasil. Ministério das Minas e Energia. Projeto Radambrasil. Folha SD. 22 Goiás: geologia, geomorfologia, pedologia, vegetação e uso potencial da terra. Rio de Janeiro; Ministério das Minas e Energia - Secretaria Geral; 1981. (Levantamento de Recursos Naturais, 25).

Cardoso MRD, Marcuzzo FFN, Barros JR. Classificação climática de Köppen-Geiger para o estado de Goiás e o Distrito Federal. Acta Geogr. 2014;8:40-55.

Cavalcanti Júnior EG, Medeiros JF, Melo TK, Sobrinho JE, Bristot G, Almeida BM. Necessidade hídrica da cultura do girassol irrigado na chapada do Apodi. R Bras Eng Agric Ambiental. 2013;17:261-7. https://doi.org/10.1590/S1415-43662013000300003

Coelho MR, Vidal-Torrado P, Ladeira FSB. Macro e micromorfologia de ferricretes nodulares desenvolvidos de arenito do Grupo Bauru, Formação Adamantina. Rev Bras Cienc Solo. 2001;25:371-85. https://doi.org/10.1590/S0100-06832001000200013

Daniels RB, Perkins HF, Hajek BF, Gamble EE. Morphology of discontinuous phase plinthite and criteria for its field identification in the southeastern United States. Soil Sci Soc Am J. 1978;42:944-9. https://doi.org/10.2136/sssaj1978.03615995004200060024x

Donagema GK, Campos DVB, Calderano SB, Teixeira WG, Viana JHM, organizadores. Manual de métodos de análise do solo. 2. ed. rev. Rio de Janeiro: Embrapa Solos; 2011.

Driessen PM, Dudal R. The major soils of the world: lecture notes on their geography, formation, properties and use. Wageningen: Agricultural University Wageningen; 1991.

Duarte MN, Curi N, Pérez DV, Kämpf N, Claessen MEC. Mineralogia, química e micromorfologia de solos de uma microbacia nos tabuleiros costeiros do Espírito Santo. Pesq Agropec Bras. 2000;35:1237-50. https://doi.org/10.1590/S0100-204X2000000600021

Inda Junior AV, Kämpf N. Variabilidade de goethita e hematita via dissolução redutiva em solos de região tropical e subtropical. Rev Bras Cienc Solo. 2005;29:851-66. https://doi.org/10.1590/S0100-06832005000600003

Instituto Brasileiro de Geografia e Estatística - IBGE. Manual técnico de pedologia. 3. ed. Rio de Janeiro: IBGE; 2015.

Ker JC. Latossolos do Brasil: uma revisão. Geonomos. 1997;5:17-40. https://doi.org/10.18285/geonomos.v5i1.187

Martins AKE, Schaefer CEGR, Silva E, Soares VP, Corrêa GR, Mendonça BAF. Relações solo-geoambiente em áreas de ocorrência de ipucas na planície do médio Araguaia - estado de Tocantins. R Arvore. 2006;30:297-310. https://doi.org/10.1590/S0100-67622006000200017

Miguel P, Dalmolin RSD, Pedron FA, Fink JR, Moura-Bueno JM. Caracterização de plintitas e petroplintitas em solos da Depressão Central do Rio Grande do Sul. Cienc Rural. 2013;43:999-1005. https://doi.org/10.1590/S0103-84782013005000065

Momoli RS, Cooper M. Erosão hídrica em solos cultivados e sob mata ciliar. Pesq Agropec Bras. 2016;51:1295-305. https://doi.org/10.1590/s0100-204x2016000900029

Moreira HL, Oliveira VA. Evolução e gênese de um Plintossolo Pétrico Concrecionário êutrico argissólico no município de Ouro Verde de Goiás. Rev Bras Cienc Solo. 2008;32:1683-90. https://doi.org/10.1590/S0100-06832008000400033

Santos HG, Jacomine PKT, Anjos LHC, Oliveira VA, Oliveira JB, Coelho MR, Lumbreras JF, Cunha TJF. Sistema brasileiro de classificação de solos. 3. ed. rev. ampl. Rio de Janeiro: Embrapa Solos; 2013.

Santos MC, Batista MA. Avaliações física, química e mineralógica em solos plínticos da região meio-norte do Brasil, submetidos a teste de umedecimento e secagem. Rev Bras Cienc Solo. 1996;20:21-31.

Santos RD, Lemos RC, Santos HG, Ker JC, Anjos LHC, Shimizu SH. Manual de descrição e coleta de solo no campo. 7. ed. rev ampl. Viçosa, MG: Sociedade Brasileira de Ciência do Solo; 2015.

van Wambeke A. Soils of the tropics: properties and appraisal. 2nd ed. Ithaca: Cornell University; 2002.

World Reference Base for Soil Resources - WRB: International soil classification system for naming soils and creating legends for soil maps. Food and Agriculture Organization of the United Nations. Rome: IUSS/ISRIC/FAO; 2015. (World Soil Resources Reports, 106).